Dielectric and Optical Properties of Nitrogen-Incorporated Polyethylene Films Fabricated by Plasma Polymerization

S. H. KIM, H. K. XIE, and K. C. KAO, *Materials and Devices Research Laboratory, Electrical Engineering Department, University of Manitoba, Winnipeg, Manitoba, Canada R3T 2N2*

Synopsis

The dielectric and optical properties of nitrogen-incorporated polyethylene films fabricated by radio-frequency glow discharge in ethylene-nitrogen (C_2H_4–N_2) gas mixtures have been measured for various nitrogen concentrations. The results show that the plasma-polymerized films have distinct properties from the ones based on conventional chemical polymerization. The incorporation of nitrogen in polyethylene results in an increase in breakdown strength, dissipation factor, and dielectric constant at frequencies below the optical frequency range, and in a decrease in dark conductivity, and in photoconductivity and extinction coefficient in the optical frequency range. However, the incorporation of nitrogen does not cause significant change in refractive index. The effects of the incorporation of nitrogen in polyethylene are attributed to the shallow acceptor-like traps introduced by incorporated nitrogen.

INTRODUCTION

Polymer films fabricated by plasma polymerization (or plasma synthesis) have been studied extensively in the past three decades because the films produced by this method have good adhesion to most substrate materials and durability to high temperatures and contain less pinholes,[1-4] and therefore have potential applications in many areas of electrical technology.[5] The dielectric properties of plasma-polymerized polyethylene films without and with nitrogen incorporation have been reported by several investigators.[6,7] However, their properties extended to the optical frequency range are scarce. The purpose of this article is to report some new results about the effects of the incorporation of nitrogen in polyethylene on their dielectric and optical properties.

EXPERIMENTAL

The radio-frequency glow discharge chamber shown in Figure 1 operating at 13.56 MHz was employed for the fabrication of polyethylene films incorporated with nitrogen by plasma polymerization of ethylene–nitrogen gas mixtures. The chamber consisted of a pair of parallel electrodes of 15 cm in diameter and 1 cm in thickness. The electrodes were aluminum discs covered with polyethylene film, the electrode separation being 4 cm. Prior to film deposition, the chamber was evacuated to about 10^{-6} torr for about 4 h and then high-purity (99.999%) ethylene–nitrogen mixture was led into the chamber, the operating pressure being about 1 torr. The content of nitrogen in the films was controlled by adjusting the volume ratio of N_2/C_2H_4 in the gas

Journal of Applied Polymer Science, Vol. 32, 5543–5556 (1986)
 CCC 0021-8995/86/065543-14$04.00

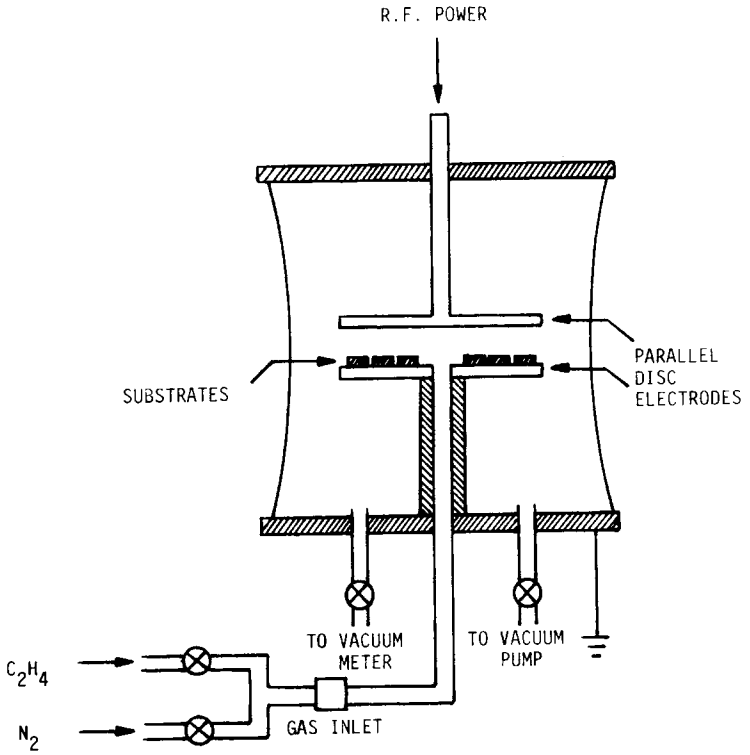

Fig. 1. Simplified schematic diagram of the radio-frequency glow discharge chamber. Embedded thermocouples and heater are not shown for clarity.

mixtures. The actual contents of nitrogen and other impurities in the films were determined using a Carlo Erba Model 1106 automatic analyzer, and the relation between the actual contents and the volume ratio are given in Table I. Thermocouples and a resistance heater were embedded beneath the bottom electrode to control and to monitor the substrate temperature, and to provide the source for heat treatment. The substrate temperature for this investigation was maintained constant at 30°C during deposition. The deposition rate was about 0.5 Å/s. After deposition, the films were kept in the chamber under a vacuum of 10^{-6} torr for heat treatment at 100°C for about 2 h in order to

TABLE I
Plasma Polymerization Parameters and Impurity Contents

Volume ratio of N_2/C_2H_4	Flow rate ($cm^3\ s^{-1}$)		Chamber pressure (torr)	Power (w)	Impurity content (wt %)			
	C_2H_4	N_2			Nitrogen	Oxygen	Carbon	Hydrogen
0	0.34	0	1	60	0.05	11.25	78.01	9.35
0.50	0.34	0.17	1	60	0.45	10.45	76.54	9.64
1.00	0.34	0.34	1	60	1.05	8.66	77.87	10.19
1.25	0.34	0.42	1	60	—	—	—	—
2.00	0.34	0.68	2	60	1.90	3.67	82.41	10.85

minimize the amount of residual free radicals and to anneal out any nonequilibrium structural stresses.

For electrical measurements, a silver layer was first vacuum-deposited on a square glass substrate of size 2.54 × 2.54 cm as the bottom electrode. After film deposition, 20 separate circular silver electrodes of diameter 0.28 cm were deposited on the polymer film surface to form the top electrodes of a sandwich configuration, the top electrode thickness being about 500 Å, suitable for self-healing breakdown measurements. The same electrode configuration was also used for dissipation factor measurements. For these measurements we had also used a three-electrode system including a guard electrode, but the measured dissipation factor is almost identical with or without the guard electrode.

For optical measurements the films were deposited on fused quartz substrates. For the absorption coefficient measurements we used a Cary Model 14 spectrophotometer, and for the refractive index and the extinction coefficient measurements we used both the Brewster-angle reflectivity and the ellipsometry techniques. In the ellipsometric measurements, we used a Gaertner type L119 ellipsometer and a Babinet-Soleil compensator in conjunction with a Bausch-Lomb grating monochromator, a mercury arc lamp, and a mica quarter-wave plate for the wavelength of 5461 Å. To avoid the light reflection from the back surface of the substrate, the back surface of each quartz substrate was ground using an abradant powder before film deposition, and after film deposition it was painted with a black paint. By null-setting the polarizer and analyzer, we could obtain two characterized parameters, defined as the phase angle change and the arctangent of the amplitude ratio change. A FORTRAN computer program was used to yield the values of the refractive index n, the extinction coefficient k, and the film thickness d by iteratively minimizing the error function.[8] Since we have only two measured parameters, we have to estimate the value of d. To minimize the computer time, it is necessary to have an accurate estimate of d.

The film thickness was determined by the following methods: (a) by means of an interferometer with the film sample covered with a vacuum deposited silver layer on the surface; (b) by weighing the substrate before and after the film deposition and calculated from the known data of the film surface area and density; and (c) by surface profile measurements. The film thickness determined by these three methods was consistent and in good agreement with that obtained from ellipsometry.

The arrangement for the Brewster angle reflectivity measurements is shown in Figure 2, which is similar to that reported by other investigators[9,10] and is self-explanatory. From a position of normal incidence (determined by the retroreflection of the incident beam) which corresponds to the point of minimum reflectance, the sample was rotated either clockwise or counterclockwise to an angle of about 3–4° less than the estimated point of minimum reflectances. Then from the curve of the relative reflectance vs. the incident angle, the point of the minimum reflectivity was determined by means of least squares curve fitting to the Fresnel's equation.[9,10] This minimum reflectivity point is the Brewster angle, from which the refractive index was calculated.

The infrared spectra were measured using a Nicolet FT-IR Model spectrometer. The films used for these measurements were deposited on NaCl

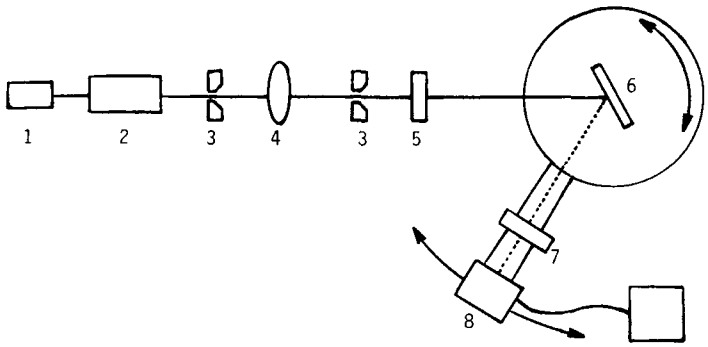

Fig. 2. Arrangement of Brewster-angle reflectance measurements: (1) mercury arc lamp; (2) monochromator; (3) slits; (4) collimating lens; (5) polarizer; (6) film sample on rotary table; (7) analyzer; (8) detector; and (9) x–y recorder.

crystal substrates which are transparent in the infrared region, and the films were made specially thick to improve the measuring accuracy.

The capacitance and the dissipation factor were measured with a General Radio Model 1615-A capacitance bridge for the frequency range from 100 Hz to 100 kHz, and with a Q-meter for the frequency range from 100 kHz to 6 MHz. The dielectric constants and the dissipation factors at 100 kHz deduced from the measurements using these two different instruments were consistent.

The breakdown voltage was measured using the well-known self-healing breakdown technique to avoid the effects of localized weak spots.[11-13] The arrangement for dc breakdown voltage measurements is shown in Figure 3. If a localized weak spot breaks down, the energy stored in the capacitor and the sample will be discharged through the weak spot and burns out the weak spot and its surrounding regions, thus healing this weak spot. It should be pointed out that an appropriate value of the capacitor, C, must be chosen for self-healing. The value of 1000 pF was used for the present investigation. Since the breakdown strength depends on the rise rate of the applied dc voltage,[14] the rise rate used for the present investigation was 5 V/s.

We used the same technique adopted by Tahira and Kao[15] for photocurrent measurements. All samples were made in a sandwich confirugation with silver

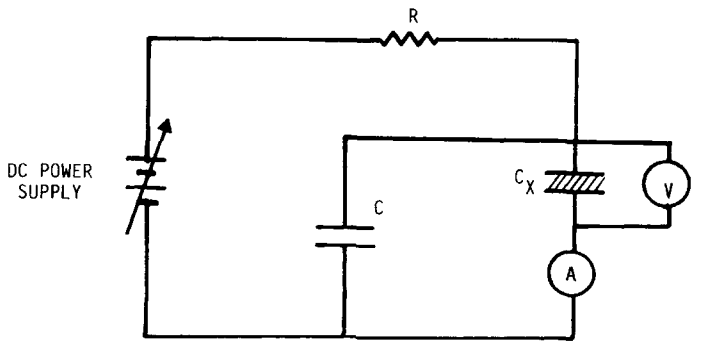

Fig. 3. Electric circuit for self-healing breakdown measurements.

vacuum-deposited on the glass substrate as the guard and the guarded electrodes prior to film deposition, and on the film surface as the illuminated electrode after film deposition, the diameter of the guarded electrode being 1.2 cm and the width of the guard electrode being 0.2 cm with a separation of 0.05 cm between these two electrodes. The front illuminated electrode on the film surface was 1.3 cm in diameter and about 200 Å in thickness, and it was transparent to the ultraviolet light used for this investigation. The ultraviolet light source was a 180 W deuterium lamp mounted in a housing with spherical mirror, lens, and slit to provide a parallel beam of size of 2 cm in diameter. For all photocurrent measurements, we used rectangular light pulses with the rise and the fall time of about 10^{-4} s produced by periodicallly chopping the illuminating beam. The pulse duration was 60 s operating at 50% duty cycle. The light intensity and the temperature of 23°C in the measuring chamber were kept constant. The dc supply was 50 V dry battery, and the currents were measured using a Keithley 610 electrometer in conjunction with a high stability Hewlett-Packard HP713-2A pen recorder. The measurement of superimposed photocurrents was carried out when a series of such light pulses was switched on to illuminate the sample through the semitransparent electrode after the elapse of 60 s from the time when a step-function dc voltage had been applied to the sample for charging or when the electrodes had been short-circuited for discharging.

We have also checked the structure of the films using a Philips X-ray diffractometer with filtered CuK_α radiation. All film samples produced for this investigation were amorphous in structure. The melting point of the plasma-polymerized films is about 210°C. which is much higher than that of the conventional polyethylene, which is about 140°C, indicating that in the plasma-polymerized films there exist short-chain molecules and a high density of crosslinks.

RESULTS AND DISCUSSION

The infrared spectra for the plasma-polymerized polyethylene films without and with nitrogen incorporation are shown in Figure 4. The CH_2 stretching band at 2900 cm^{-1}, the CH_2 bending band at 1463 cm^{-1}, and the CH_2 wagging band at 1369 cm^{-1} are similar to those in conventional polyethylene. However, in plasma-polymerized films there are no strong $(—CH_2—)_2$ vibration band at 750 cm^{-1} and bands corresponding to unsaturation such as at around 1600 and 900 cm^{-1}, which exist in conventional polyethylene. The incorporation of nitrogen in polyethylene gives rise to three new absorption bands in the vicinities of 3300, 2200, and 1600 cm^{-1}, which correspond to the stretching bands of the N=H bond, the C=N bond, and the C≡N bond, respectively.[7,16]

In general, the conventional polyethylene is a nonpolar material having a dielectric constant of about 2.2 and a dissipation factor of about 10^{-4} independent of frequency in the frequency range from 100 Hz to 1 MHz. However, the plasma-polymerized films have a dielectric constant of about 3 and a dissipation factor strongly dependent on frequency. This is mainly due to the fact that the plasma-polymerized films contain various free radicals such as the hydroxyl and carbonyl groups, which are polar in nature. Figures 5

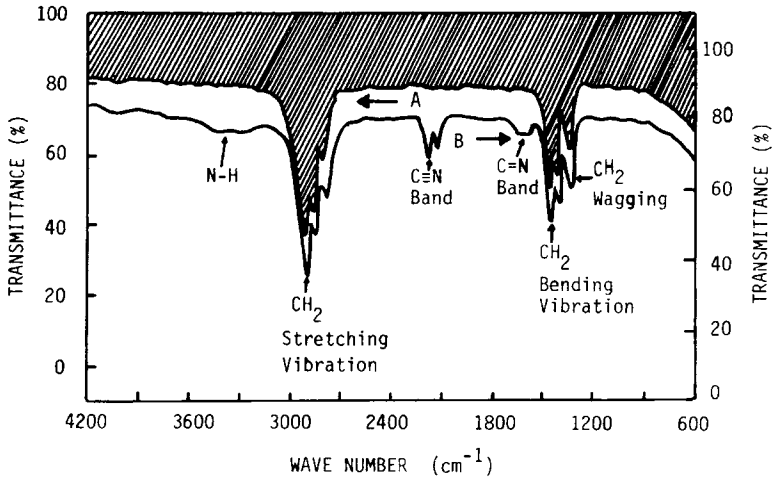

Fig. 4. The infrared spectra of plasma-polymerized polyethylene films: (A) without nitrogen incorporation and (B) with nitrogen incorporation.

and 6 show the frequency dependence of the dielectric constant and the dissipation factor for films without and with nitrogen incorporation, and without and with heat treatment. The exposure of the films to air results in a higher dissipation factor because of oxygen trapped in the films. On the basis of their ESCA and ESR measurements Hozumi et al.[17] have reported that the plasma-polymerized polyethylene films trap oxygen rapidly when they are

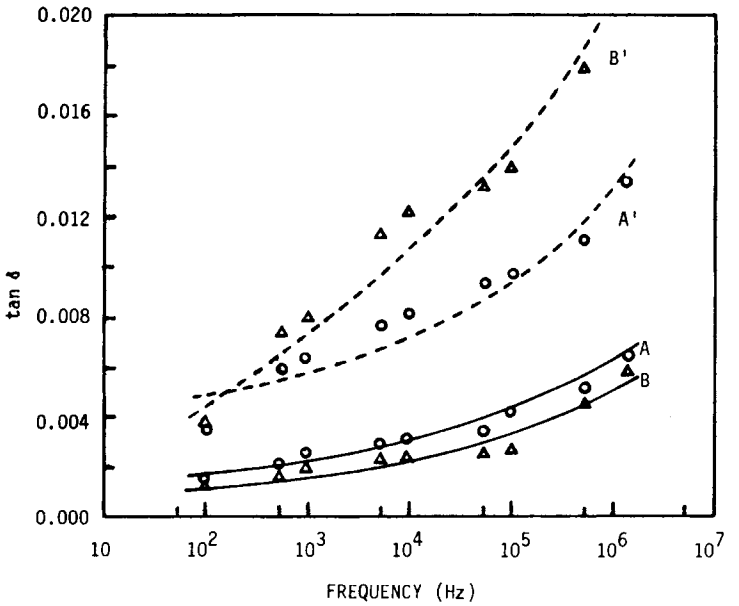

Fig. 5. The effect of exposure of the plasma polymerized films in air on the dissipation factor-frequency characteristics. (The films were not subjected to heat treatment after deposition): (A) volume ratio of $N_2/C_2H_4 = 0$, exposure time = 1 h; (A′) volume ratio of $N_2/C_2H_4 = 0$, exposure time = 3 weeks; (B) volume ratio of $N_2/C_2H_4 = 0.5$, exposure time = 1 h; (B′) volume ratio of $N_2/C_2H_4 = 0.5$, exposure time = 3 weeks.

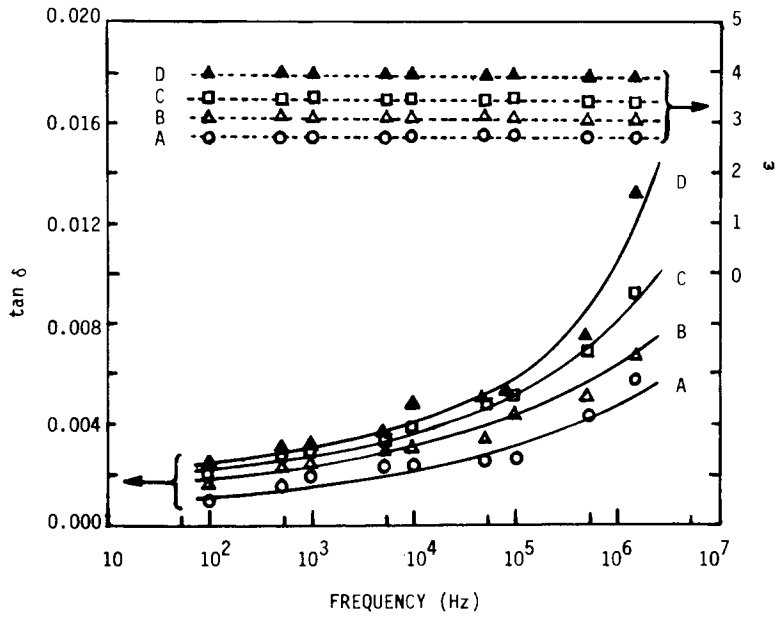

Fig. 6. The dielectric constant and the dissipation factor as functions of frequency for plasma polymerized polyethylene films deposited at the gas mixture with the volume ratio of N_2/C_2H_4 of: (A) 0; (B) 0.5; (C) 1; (D) 1.25. The films were subjected to heat treatment but without exposure to air after deposition.

exposed to air after polymerization, and that the free radicals tend to combine with oxygen atoms in the films. The heat treatment under high vacuum reduces the amount of residual free radicals and anneals out structural stresses, thus resulting in a decrease in dissipation factor as shown in Figures 5 and 6. The incorporation of nitrogen in the films introduces N=H, C=N, and C≡N terminals, which are polar in nature. It can also be expected that the higher the nitrogen content, the higher are the dielectric constant and the dissipation factor as shown in Figures 5 and 6.

The average breakdown strength of the plasma-polymerized films increases with increasing nitrogen content as shown in Figure 7, and also increases with decreasing film thickness for film thicknesses lower than 0.5 μm as shown in Figure 8. On the basis of Kao's model for electric breakdown in low-mobility condensed materials,[18] the increase in breakdown strength due to the nitrogen incorporation may be associated with the creation of shallow traps in the energy gap by the incorporated nitrogen. These shallow traps act as stepstones, tending to reduce the energy released due to trapping or recombination processes, and hence reducing the energy of hot electrons produced by an Auger-type process. This chain action in turn reduces the probability for the formation of low density domains, thus increasing breakdown strength.

The absorption coefficient α measured with a spectrophotometer as a function of photon energy for the films without and with nitrogen incorporation is shown in Figure 9. The extinction coefficient k deduced from Figure 9 based on the relation $k = \alpha\lambda/4\pi$, where λ is the light wavelength, and the refractive index n deduced from the Brewster angle reflectivity measurements are shown in Figure 10. We have also measured n and k using an ellipsome-

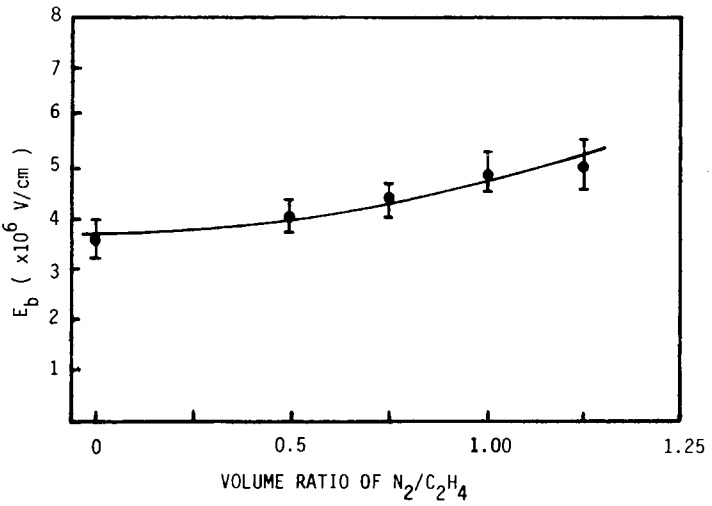

Fig. 7. Average breakdown strength of plasma polymerized polyethylene films E_b as a function of gas mixture volume ratio of N_2/C_2H_4.

ter. The results for n and k are practically identical to those deduced from the Brewster-angle reflectivity and spectrophotometric measurements. From the values of n and k given in Figure 10, we also have calculated the complex dielectric constant using the following relations: $\epsilon' = n^2 - k^2$ and $\epsilon'' = 2nk$. The real part ϵ' and the imaginary part ϵ'' of the complex dielectric constant as functions of photon energy are shown in Figure 11

It is interesting to note that the refractive index is not sensitive to nitrogen incorporation and photon energy for photon energies up to 3.6 eV. Because of the limitation of our experimental systems, we could not measure n beyond 3.6 eV. However, n is expected to increase with increasing photon energy beyond 3.6 eV because of the increase of the contribution of excited free

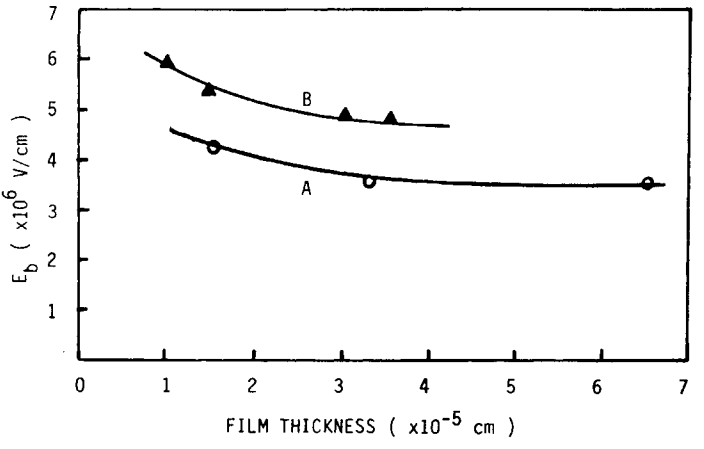

Fig. 8. Average breakdown strength as a function of film thickness for the plasma polymerized polyethylene films: (A) without nitrogen incorporation and (B) with nitrogen incorporation (volume ratio of N_2/C_2H_4 = 1.25).

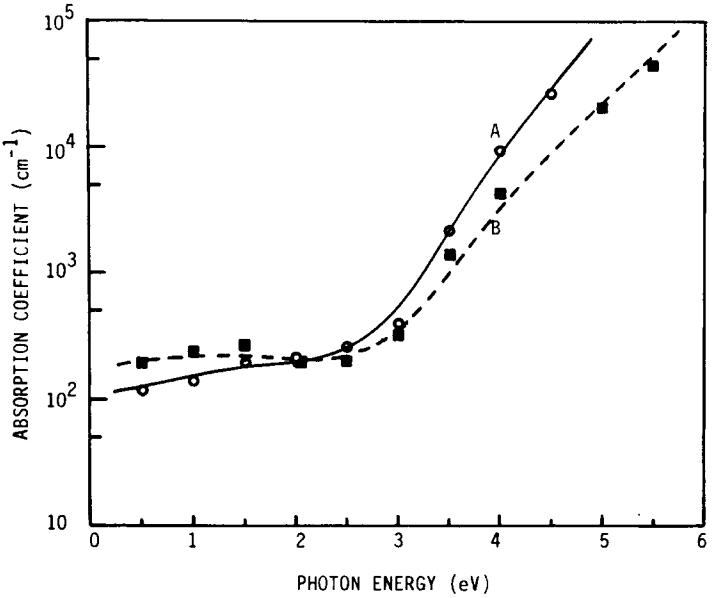

Fig. 9. Absorption coefficient of plasma polymerized polyethylene films as a function of photon energy: (A) volume ratio of $N_2/C_2H_4 = 0$; (B) volume ratio of $N_2/C_2H_4 = 2$.

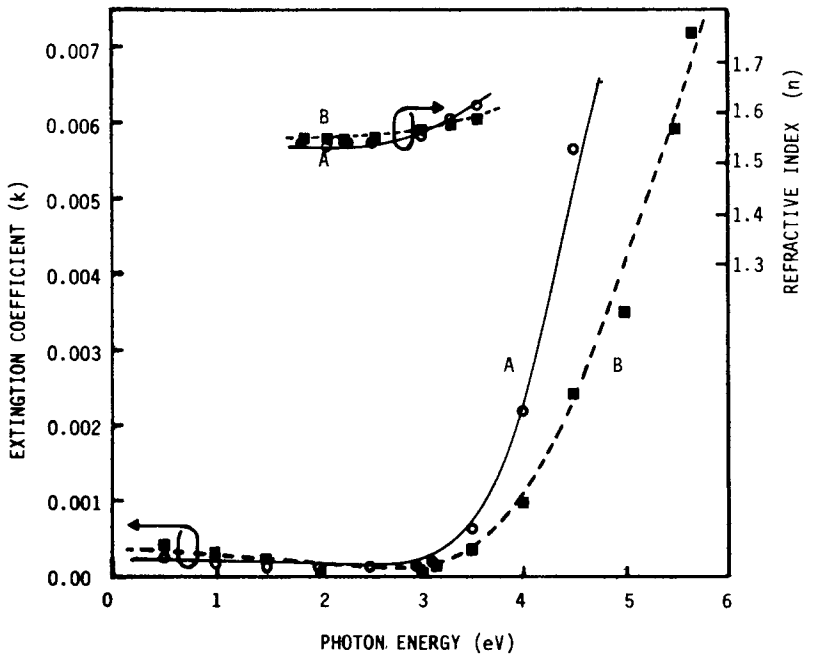

Fig. 10. Refractive index n and extinction coefficient k of plasma-polymerized polyethylene films as functions of photon energy: (A) volume ratio of $N_2/C_2H_4 = 0$ and (B) volume ratio of $N_2/C_2H_4 = 2$.

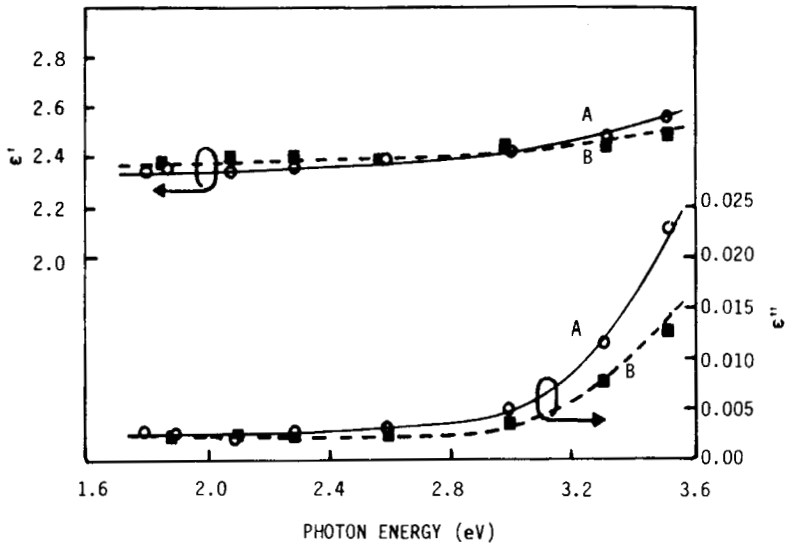

Fig. 11. Real part (ϵ') and imaginary part (ϵ'') of the complex dielectric constant as functions of photon energy for plasma polymerized polyethylene films: (A) volume ratio of $N_2/C_2H_4 = 0$; (B) volume ratio of $N_2/C_2H_4 = 2$.

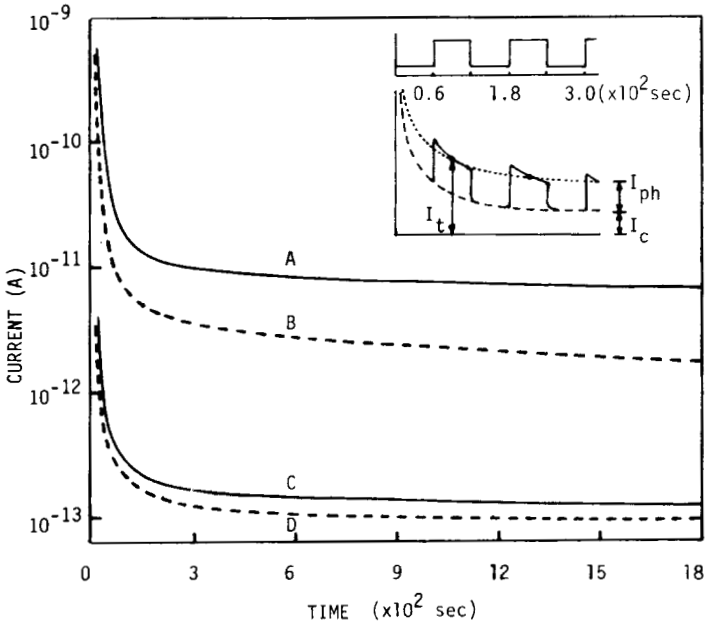

Fig. 12. The total current (I_t) consisting of the photocurrent (I_{ph}) superimposed onto the charging current (I_c) under exciting radiation by ultraviolet light pulses for the illuminated electrode positively biased at 0.45 MV/cm: (A) total current I_t of films (volume ratio of $N_2/C_2H_4 = 0$); (B) dark charging current I_c of films (volume ratio of $N_2/C_2H_4 = 0$); (C) total current I_t of films (volume ratio of $N_2/C_2H_4 = 1$); (D) dark charging current I_c of films (volume ratio of $N_2/C_2H_4 = 1$).

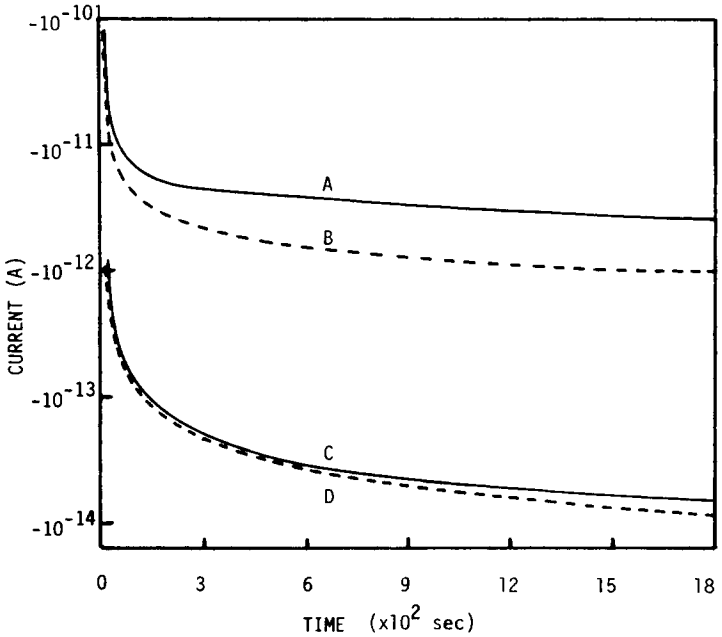

Fig. 13. The total current (I_t) consisting of the photocurrent (I_{ph}) superimposed onto the discharging current (I_d) under exciting radiation by ultraviolet light pulses for the illuminated electrode originally positively biased at 0.45 MV/cm prior to short-circuiting the electrodes: (A) total current I_t (volume ratio of $N_2/C_2H_4 = 0$); (B) dark discharging current I_d (volume ratio of $N_2/C_2H_4 = 0$); (C) total current I_t (volume ratio of $N_2/C_2H_4 = 1$); (D) dark discharging current I_d (volume ratio of $N_2/C_2H_4 = 1$).

carriers. The extinction coefficient k for the films with nitrogen incorporation is slightly higher than that without for photon energies lower than 2.4 eV, but this trend is reversed for photon energies higher than 2.4 eV as shown in Figure 10. In the optical frequency range the contribution of both bound and free carriers must be considered. For photon energies lower than 2.4 eV the contribution of bound electrons may be predominant. However, for photon energies higher than 2.4 eV the contribution of excited free carriers becomes predominant. As shown in Figures 12–15, the photocurrent is much higher for the films without than with nitrogen incorporation because of the new traps created by the incorporated nitrogen. It is thus expected that the higher the dark conductivity and the photoconductivities, the more are the free carriers and hence the higher is the value of k.

By taking the photocurrent measured at the middle of the photocurrent pulse as the mean pulsed photocurrent, the total current I_t is the sum of the dark current (charging, I_c, or discharging, I_d) and the mean photocurrent I_{ph} as illustrated in Figure 12. The charging current I_c was measured after the application of a step-function dc voltage and the discharging current I_d was measured after the removal of the applied voltage and the short-circuiting of the guarded and the illuminated electrodes. Both I_t and I_c (or I_d) decay with time as shown in Figures 12 and 13 for the positively biased electrode illuminated by a series of ultraviolet light pulses, and those in Figures 14 and 15 for the negatively biased electrode illuminated by a series of ultraviolet

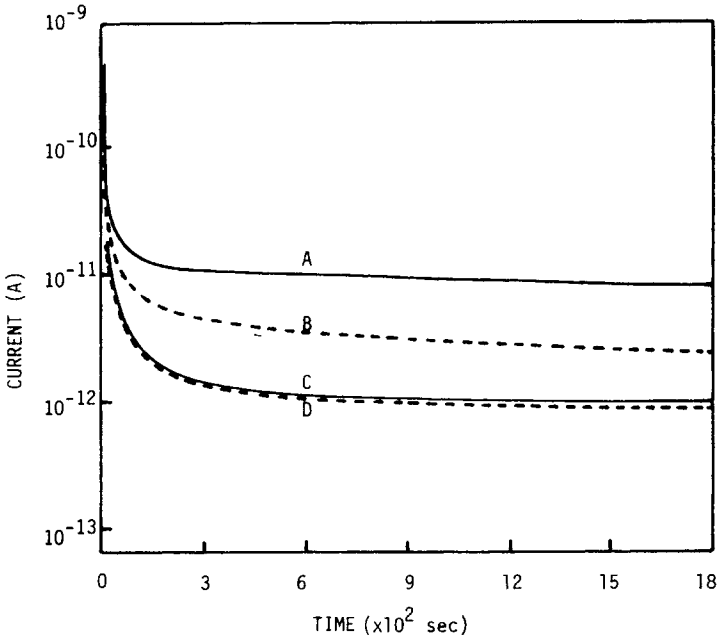

Fig. 14. The total current (I_t) consisting of the photocurrent (I_{ph}) superimposed onto the charging current (I_c) under exciting radiation by ultraviolet light pulses for the illuminated electrode negatively biased at 0.45 MV/cm: (A) I_t (volume ratio of $N_2/C_2H_4 = 0$); (B) I_c (volume ratio of $N_2/C_2H_4 = 0$); (C) I_t (volume ratio of $N_2/C_2H_4 = 1$); (D) I_c (volume ratio of $N_2/C_2H_4 = 1$).

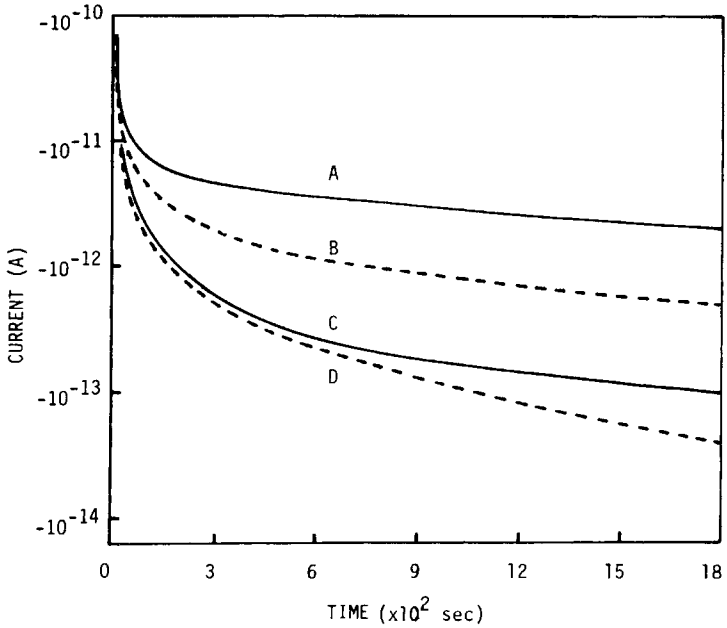

Fig. 15. The total current (I_t) consisting of the photocurrent (I_{ph}) superimposed onto the discharging current (I_d) under exciting radiation by ultraviolet light pulses for the illuminated electrode originally negatively biased at 0.45 MV/cm prior to short-circuiting the electrodes: (A) I_t (volume ratio of $N_2/C_2H_4 = 0$); (B) I_d (volume ratio of $N_2/C_2H_4 = 0$); (C) I_t (volume ratio of $N_2/C_2H_4 = 1$); (D) I_d (volume ratio of $N_2/C_2H_4 = 1$).

light pulses. For the films without nitrogen incorporation, the dark current (charging or discharging) and the photocurrent for the illuminated electrode positively biased are almost identical to those for the illuminated electrode negatively biased. This implies that the film sample is so thin that the absorption in the bulk is reasonably uniform, unlike the results of Tahira and Kao,[15] who observed a strong polarity effect for thick conventional polyethylene of 20 μm in thickness. However, for the films with nitrogen incorporation, there is a strong polarity effect and the photocurrent is very small. The incorporation of nitrogen in polyethylene in general reduces both the dark current and the photocurrent, but such a reduction is much larger for the illuminated electrode positively biased than that with the illuminated electrode negatively biased. This phenomenon is attributed to the shallow acceptorlike traps created by the incorporated nitrogen, which may be Gaussianly distributed and located between the conduction band and the original acceptorlike traps existing in the films without nitrogen incorporation. We believe that the dark conduction is mainly due to electron transport, and the decay during the charging period is associated with the time-dependent trap-filling by injected electrons, and the decay during the discharging period is associated with the time-dependent thermal release of trapped electrons. According to the model put forward by Tahira and Kao,[15] the photocurrent is mainly the hole current. The ultraviolet light radiation produces mainly trapped electrons and free holes. The higher the density of the acceptorlike traps, the shorter is the hole lifetime because the filled acceptorlike traps are the most effective hole traps. This is why the photocurrent is very small in the films incorporated with nitrogen.

CONCLUSIONS

On the basis of the experimental results described above, the following conclusions are drawn:

1. The dark charging current is associated with the electron injection and the trap-filling processes, and the dark discharging current is associated with the thermally activated detrapping processes.
2. The electrons trapped in the acceptorlike traps (filled traps) act most effectively as deep traps for holes.
3. The photocurrent is mainly due to hole transport.
4. The dielectric losses in the optical frequency range is mainly due to excited free carriers.
5. The increase in breakdown strength with increasing nitrogen content in the polyethylene films is attributed to the shallow traps created by the incorporated nitrogen, which reduces the energy of the hot electrons produced by an Auger-type process, thus reducing the probability for the formation of low-density domains. This phenomenon is in support of Kao's model of electric breakdown in low mobility condensed insulators.

We wish to thank F. Y. Liu, D. Liu, S. R. Mejia, H. C. Tse, V. Herak, and K. Ahmed for technical assistance, and the Natural Sciences and Engineering Research Council of Canada for supporting this research under Grant A-3339.

References

1. E. G. Linder and A. P. Davis, *J. Phys. Chem.*, **35**, 3649 (1931).
2. H. Kobayashi, A. T. Ball, and M. Shen, *J. Appl. Polym. Sci.*, **17**, 885 (1973).
3. H. Yasuda and T. Hirotsu, *J. Polym. Sci., Polym. Chem. Ed.*, **16**, 743 (1978).
4. M. Shen and A. T. Bell, *Plasma Polymerization*, ACS Symp. Ser. 108, Am. Chem. Soc., Washington, DC, 1979.
5. Y. Sequi, B. Ai, and H. Carchano, *J. Appl. Phys.*, **47**, 140 (1976).
6. N. Hozumi, T. Takao, and Y. Ohki, *Jpn. J. Appl. Phys.*, **21**, L195 (1982).
7. M. Hudis and T. Wydeven, *J. Polym. Sci., Polym. Lett. Ed.*, **13**, 549 (1975).
8. F. L. McCrackin, NBS Technical Note 479, 1969.
9. M. S. Walen and J. Stone, *J. Appl. Phys.*, **53**, 4340 (1982).
10. H. E. Bennett and J. M. Bennett, in *Physics of Thin Films*, G. Hass and R. E. Thun, Eds., Academic, New York, 1967, Vol. 4, pp. 1–90.
11. M. Hikita, A. Matsuda, M. Nagao, G. Sawa, and M. Ieda, *Jpn. J. Appl. Phys.*, **21**, 475 (1982).
12. N. Klein, *IEEE Trans. Electron Devices*, **ED-13**, 788 (1966).
13. S. Sapieha, M. R. Wertheimer, and A. Yelon, *IEEE Trans. Elec. Insul.*, **EI-14**, 229 (1979).
14. M. Hikita, A. Matsuda, M. Nagao, G. Sawa, and M. Ieda, *Jpn. J. Appl. Phys.*, **21**, 483 (1982).
15. K. Tahira and K. C. Kao, *J. Phys. D: Appl. Phys.*, **18**, (1985).
16. J. Bellamy, *The Infrared Spectra of Complex Molecules*, 2nd ed., Metheun, London, 1958.
17. N. Hozumi, T. Takao, Y. Kasama, and Y. Ohki, *Jpn. J. Appl. Phys.*, **22** 636 (1983).
18. K. C. Kao, *J. Appl. Phys.*, **55**, 752 (1984).

Received December 16, 1985
Accepted February 7, 1986